Front. Phys. 10, 107801 (2015)
DOI 10.1007/s11467-015-0491-z

RESEARCH ARTICLE

Effect of thermal annealing on sub-band-gap absorptance of microstructured silicon in air

Li-Ping Cao (曹丽萍)[1,2,*], **Zhan-Dong Chen** (陈战东)[1], **Chun-Ling Zhang** (张春玲)[1], **Jiang-Hong Yao** (姚江宏)[1,†]

[1] *The MOE Key Laboratory of Weak Light Nonlinear Photonics, TEDA Applied Physics Institute and School of Physics, Nankai University, Tianjin 300457, China*

[2] *Department of Physics, Kashgar Teachers College, Kashgar, Xinjiang 844000, China*

Corresponding authors. E-mail: [*] *caolp2778@163.com,* [†] *yaojh@nankai.edu.cn*

Received January 21, 2015; accepted May 3, 2015

The optical absorption properties of femtosecond-laser-made "black silicon" as a function of the annealing conditions were investigated. We found that the annealing process changes the surface morphology and absorption spectroscopy of the "black silicon" samples, and obtained a maximum sub-band-gap absorptance value of approximately 30% by annealing at 1000 °C for 30 min. The thermal relaxation and atomic structural transformation mechanisms are used to describe the lattice recovery and the increase and decrease of the substitutional dopant atom concentration in the microstructured surface during the annealing. Our results confirm that: i) owing to the thermal relaxation, the lattice defects decrease with the increase of the annealing temperature; ii) the quasi-substitutional and interstitial configurations of the doped atoms transform into substitutional arrangements when the annealing temperature increases; iii) the quasi-substitutional and interstitial configurations with higher energies of the doped atoms transform into interstitial configurations with the lowest energy after high-temperature annealing for a long period of time, causing the deactivation or reactivation of the sub-band-gap absorptance by diffusion. The results demonstrate that the annealing can improve the properties of "black silicon", including defects repairing, carrier lifetime lengthening, and retention of a high absorptive performance.

Keywords sub-band-gap absorptance, black silicon, annealing, diffusion

PACS numbers 78.40.-q, 81.15.Fg, 81.40.Ef, 66.30.-h

Frontiers of Physics

1 Introduction

Recently, owing to the importance of developing silicon-based optoelectronic integration devices, micro and nanoscale silicon materials (such as microstructured silicon) have attracted increasing attention. However, the high reflection of the silicon surface in the visible to infrared region and the band gap of 1.12 eV cause low absorptance in the visible to near-infrared region, especially for wavelengths longer than 1.1 μm. The optics related applications of silicon materials are therefore limited.

In 1998, Eric Mazur's group obtained microstructured black silicon (b-Si) [1] whose light absorption in the wavelength range of 250–2500 nm exceeded 90% after irradiating silicon with a femtosecond laser [2]. Since then, several studies have been conducted on the properties of microstructured silicon [3–11]. The photocarrier production of the microstructured area is at least three times as that of the unstructured area for a bias voltage of 900 V or greater [12, 13]. Therefore, b-Si is an amazing material with potential application in the field of silicon-based optoelectronic devices including novel detectors, sensors [14], and solar cells [15]. In addition, the thermal effect is inhibited by the ultrafast femtosecond laser processing, and a plasma plume, which includes a large number of silicon species, is formed and ejected [16]. As a result, the lattice surfaces are badly damaged, and a large number of surface defects are produced, causing a significant suppression of the carrier mobility. Therefore, microstructured silicon materials need to be treated to optimize their qualities, and annealing is a widely adopted method to improve the performance of micro and nanoscale silicon materials [17, 18]. Annealing can

© Higher Education Press and Springer-Verlag Berlin Heidelberg 2015

alter the photoelectric properties of b-Si, such as the photoluminescence efficiency [19, 20], the optical response [21, 22], and especially the near infrared absorption of b-Si, as Aziz [23], Mazur [12, 24–28], and Zhuang [29] *et al.* have demonstrated. However, the optimal annealing conditions still need to be carefully determined, and the physical mechanism of the annealing process in the complex system of micro and nanoscale materials requires further investigations, as it is currently quite unclear.

In this letter, we report our annealing results on the change of the sub-band-gap absorptance of b-Si fabricated by femtosecond laser in air. By analyzing the change of the surface morphology of b-Si after annealing and its optical characteristics for different annealing temperatures and time durations, we investigated the influence of the annealing conditions on the b-Si optical properties to explore the obscure physical mechanisms and further develop the b-Si optoelectronic performance.

2 Research methods

The b-Si samples were prepared by Ti: sapphire femtosecond laser irradiation in air with a pulse duration of 120 fs and a 1 kHz repetition rate at the central wavelength of 800 nm. In the used setup, the laser beam passes through a half-wave plate and a Glan–Taylor polarizer, and it is then vertically focused on a silicon wafer by a lens with a focal length of 0.5 m. The used silicon wafers had an n-type silicon (100) surface and a resistivity of more than 2000 Ω·cm, which is fixed on a sample holder catched by a three-axis magnetic translation stage. By setting a scan speed of 0.25 mm/s and an interval of 50 μm between the scan lines of the incident laser beam, modulating the intensity of the incident laser beam, and changing the distance between the lens and the silicon wafer, we obtained an optimal laser spot size of 150 μm in diameter on the silicon wafer to fabricate 12 mm × 12 mm microstructured b-Si samples with a laser fluence of 10.0 kJ/m^2.

The samples were annealed in vacuum using an OTF-1200X-type high-temperature sintering furnace with a vacuum tube, which is evacuated by a 2TW-4C-type vacuum pump with a twin-stage sliding rotary vane. We set nine different vacuum annealing conditions covering a matrix of three temperatures (600 °C, 800 °C, 1000 °C) and three times (30 min, 180 min, 300 min) for the b-Si samples. The temperature-time control programs for the 30 min annealing process are shown in Fig. 1; the programs for the 180 min and 300 min annealing processes are similar.

Field-emission scanning electron microscopy (FE-SEM, 1530VP) was used to obtain the surface morphology of the samples before and after annealing.

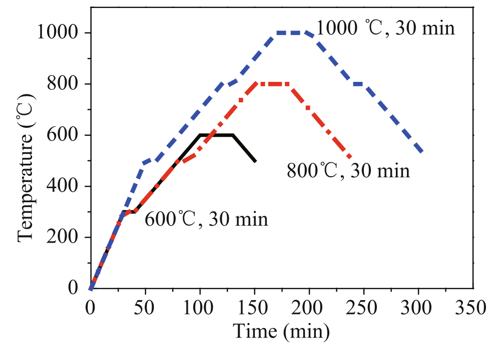

Fig. 1 Temperature-time control programs for the 30 min annealing process.

We measured the reflectance R and transmittance T in the visible-near infrared region (400–2500 nm) before and after annealing using an AVASPEC spectrometer equipped with a spherical detector. Then, the absorptance of the samples was obtained by using the formula: $A = 1 - R - T$.

3 Results and discussion

After annealing, a change of both the surface morphology and the optical properties of b-Si was observed. By analyzing the change, especially the variation of the optical absorptance at different annealing temperatures and time durations, we investigated the effect of the annealing process on the sub-band-gap absorptance to gain useful information on the annealing mechanism.

After being irradiated by the femtosecond laser, the initially bright and smooth surface of the crystalline silicon (c-Si) wafer assumed a dark gray color. The SEM images of the unannealed and annealed b-Si samples are shown in Fig. 2. Quasi-ordered arrays of blunt spikes with a size of approximately 10 μm were formed [see Fig. 2(a) and its inset i] on the silicon surface. The blunt spikes were covered with two types of particles: the first type included particles with a size of a few hundred nanometers, while the other type included particles with a size smaller than 100 nm. The latter formed a net-like structure of clusters [see Fig. 2(a) and its inset ii]. The blunt spikes did not clearly change after annealing in vacuum, but the net-like structure of the clusters was greatly reduced [see Fig. 2(b) and its inset].

Ultrafast melting and ablation occur on the silicon surface during the femtosecond laser irradiation in air at the incident fluence of 10 kJ/m^2, which is slightly above the threshold of the plasma formation [16]. As a result, plasma plume, which includes silicon ions, silicon atoms,

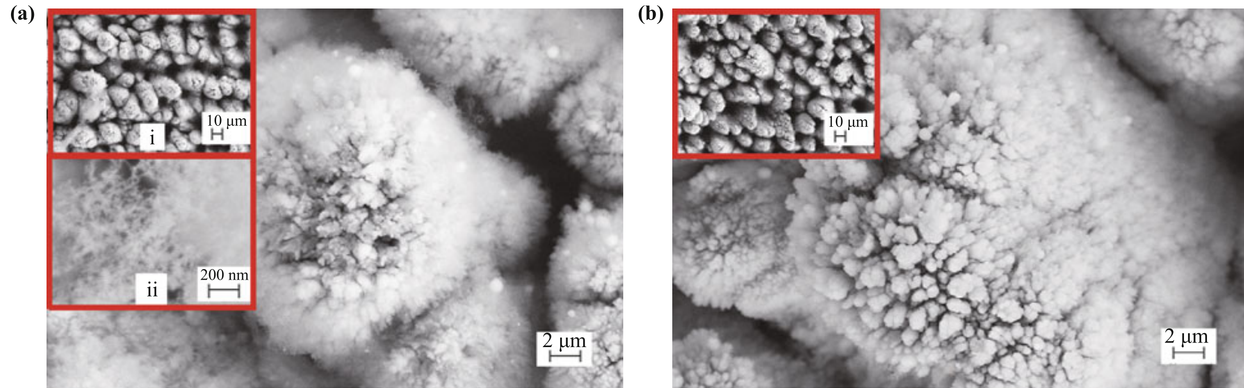

Fig. 2 Scanning electron microscopy images of b-Si samples **(a)** before annealing and **(b)** after annealing in vacuum. The insets show the surface at higher resolution.

SiO_2 molecules, and silicon nanoparticles, is expelled fleetly from the silicon surface. The removed material plume can redeposit on the etched surface because of the confinement of the ambient gas, leading to the formation of net-like clusters of nanoparticles. The laser irradiation heats and then melts the surface, causing the diffusion of oxygen into the silicon substrate and enhancing the oxidation. The resolidification of the melted layer occurs at the solid/liquid interface, forming a layer of Si-rich SiO_x $(0 < x < 2)$, i.e., an amorphous and polycrystalline layer that contains many silicon nanoclusters embedded in a SiO_2 matrix of submicrometer scale. This layer incorporates a large number of dangling bonds, oxygen-related defects, and lattice-damaged defects. During the annealing in vacuum, the adsorbed net-like nanoparticle clusters of silicon and SiO_2 melt, desorb, and diffuse into the amorphous and polycrystalline layer, dangling bonds, and lattice defects on the surface of the blunt spikes, and the Si/SiO_2 interface is restored. This result is consistent with the observation that annealing in vacuum leads to the decrease and even disappearance of the net-like micro and nanostructures.

To quantitatively analyze the variation of the optical properties, we measured the reflectance and transmittance of c-Si and b-Si before and after annealing, and then calculated the absorptance corresponding to such values of reflectance and transmittance, as shown in Fig. 3. Obviously, the absorptance of the unannealed b-Si is higher than that of c-Si and decreases monotonously with the increase of the wavelength in the range of 400–2500 nm. The absorptance of b-Si decreases after annealing, especially in the near-infrared region. However, it is still higher than that of c-Si, and varies not only with the wavelength, but also with the annealing conditions. Remarkably, the dependence of the absorptance on the annealing conditions between approximately 1200 and 1500 nm is different from that in the region between 1500 and 2500 nm.

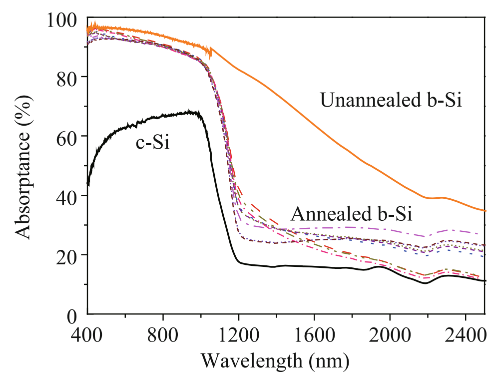

Fig. 3 Absorptance of c-Si, unannealed b-Si, and annealed b-Si.

The b-Si surface is covered with nanoparticles, an amorphous layer, and various defects. The presence of defects, impurities, different crystalline phases, and different orientation of the grains might cause the scattering of light, leading to a decrease in transmission. The micro and nanostructures on the b-Si surface cause multiple reflections of the incident light, leading to an increase of the absorptance and the decrease of the reflectance, i.e., to light trapping. The band gap of 1.12 eV determines the low absorption of crystalline silicon at wavelengths longer than 1100 nm. However, by melting, ablation, and resolidification, owing to the presence of mid-gap energy levels or bands of the defects and impurities in the band gap of silicon, as well as the light trapping structures, a substantial increase of the near-infrared absorption is achieved for b-Si. During the annealing in vacuum, the diffusion of oxygen atoms on the b-Si surface and the lattice relaxation cause the reduction of dangling bonds and lattice-damaged defects, resulting in the decrease of the state densities on the silicon surface and Si/SiO_2 interface. Owing to the decrease of the state densities of the mid-gap bands, this phenomenon suppresses the sub-band-gap absorptance of annealed b-Si.

The absorptance of b-Si barely changes under different annealing conditions for wavelengths shorter than 1100 nm (see Fig. 3). Hence, we focus on sub-band-gap absorption in the region above 1100 nm. To analyze the effect of the annealing on the optical properties of b-Si, we investigated the sub-band-gap absorptance of the samples annealed in different conditions. The dependences of the optical properties on the annealing temperature and annealing time were studied.

The higher sub-band-gap absorptance of b-Si most likely derives from the higher density of impurities and lattice defects. The impurities introduce some states both near the band edge and in the middle of the band gap of silicon, while the lattice defects introduce some states near the band edge and then form the band-tail localized states. Therefore, we assume that the absorption in the range of roughly 1200–1500 nm originates from the transition of the electrons from the top of the valence band to the band-tail localized states near the bottom of the conduction band, from the band-tail localized states near the top of the valence band to the bottom of the conduction band, or between both the band-tail localized states. Conversely, the absorption in the region above 1500 nm is attributed to the transitions of the electrons between the top of the valence band or the bottom of the conduction band and the mid-gap impurities bands on the b-Si surface.

Previous research demonstrated that the annealing of doped silicon may cause the deactivation [12, 23, 25, 28, 29] or reactivation [26] of the sub-band-gap absorptance. The damage and disorder introduced in the lattice by the femtosecond laser irradiation and the incorporation of the background gas create a tail of states below the band gap and form new electronic configurations. The thermal relaxation of the disordered silicon network makes the electronic structure partially revert to crystalline silicon, leading to the narrowing of the band tail and to a lower number of available states; thus, the lattice defects decrease with the increase of the annealing temperature. Consequently, the absorptance of b-Si in the range of roughly 1200–1500 nm decreases, causing the increase of the reflectance and transmittance with the annealing temperature, as shown in Figs. 4(a), (b), and their insets. Here, the annealing causes the deactivation of the sub-band-gap absorptance, but, as the thermal relaxation occurs in a very short time [30], the reflectance, transmittance, and absorptance do not exhibit any variation for different annealing time durations, as shown in Figs. 5(a), (b), and their insets.

To explain the influence of the annealing temperature on the optical absorptance of b-Si in the region above 1500 nm, we consider the structural transformations of

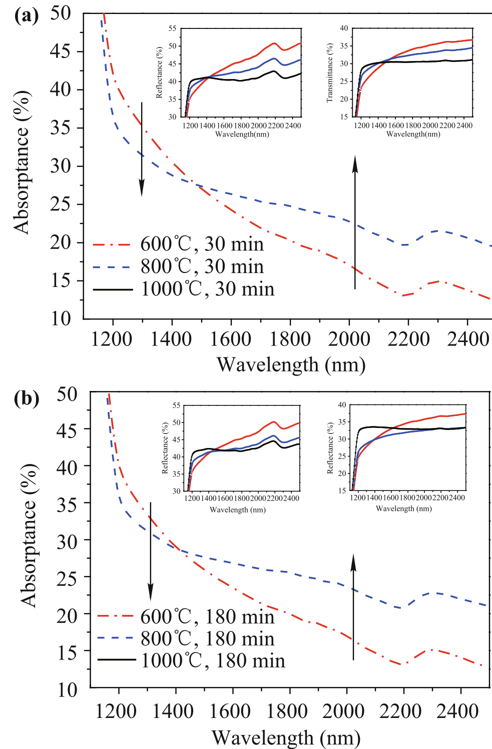

Fig. 4 Sub-band-gap absorptance of the samples annealed at different temperatures for uniform time of **(a)** 30 min and **(b)** 180 min. The results for the 300 min annealed sample are not shown as they are similar to those of the 180 min sample. The reflectance and transmittance are shown in the insets.

the various structures of doped silicon from reference [29], rather than use the precipitation of the dopant at the grain boundaries from reference [25]. Despite the chalcogen dopants in reference [29], here, O belongs to the same family of S, Se, and Te, and they are comparable because of the similar atomic structure and the same valence-electron configuration. Through the ultrafast and ultrastrong interactions of the femtosecond laser with the silicon materials in air, very rich structures are formed, in which the oxygen atoms could occupy various positions, i.e., so-called interstitial, quasi-substitutional, and substitutional configurations with diverse structural characteristics. These three configurations are proportionally distributed with different relative percentages. Except for the interstitial atoms that lie in the lowest energy states, most of the other configurations can generate defect states in the band gap of silicon, contributing to the sub-band-gap absorption. During the annealing, apart from the O–Si bonds of oxygen atoms combined with the dangling bonds on the surface of b-Si, the diffusion of the oxygen atoms causes the transformation of the geometric configurations of atomic structures with higher energies into those with lower energies, which include the lowest interstitial states, substitutional states, or quasi-substitutional states. The diffusion of the inter-

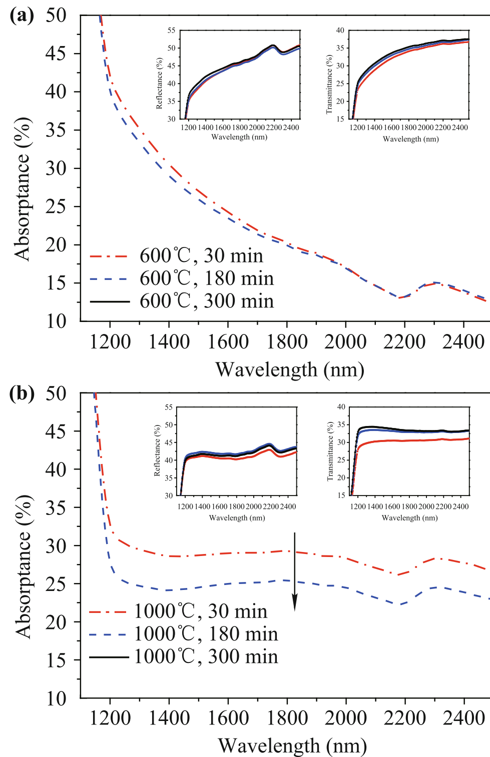

Fig. 5 Sub-band-gap absorptance of the samples annealed at identical temperatures and different times: **(a)** 600 °C, **(b)** 1000 °C. The results for the sample annealed at 800 °C are not shown as they are similar to those of the sample annealed at 600 °C. The reflectance and transmittance are shown in the insets.

stitial Si atom away from the impurity is facilitated by the increase of the annealing temperature, which causes the transformation from quasi-substitutional to substitutional configuration. Meanwhile, the active oxygen atoms might become stably bonded with silicon at higher temperature, resulting in the transformation from interstitial to substitutional configuration. Thus, the concentration of substitutional oxygen atoms, which plays an important role in the optical absorption, will increase as the annealing temperature increases. Therefore, the light absorptance in the region above 1500 nm increases with the annealing temperature, while the reflectance and transmittance decrease, as shown in Figs. 4(a), (b), and their insets. The result indicates that the absorptance in the region above 1500 nm is reactivated through high-temperature annealing.

To support our speculations, micro-Raman analysis was conducted to detect the changes in the b-Si lattice. Raman spectroscopy is sensitive to atomic arrangements and phonon modes in solids. The Raman spectra of unannealed b-Si and b-Si after 30, 180, and 300 min of annealing at 600, 800, and 1000 °C are shown in Fig. 6 and its inset, revealing the phase transformations of b-Si and providing some insights to our observed sub-band-gap absorptance. Silicon transforms from its diamond cubic phase (Si-I) to silicon with an R8 structure (Si-XII), BC8 structure (Si-III), and amorphous silicon (a-Si) during pressure loading and unloading [27]. The ultrastrong and ultrafast action that occurs during the femtosecond laser processing produces pressure waves. Upon pressure release, silicon partly transforms from Si-I (299 cm^{-1} and 519 cm^{-1}) to Si-XII (400 cm^{-1}) and Si-III (387 cm^{-1}). In the meanwhile, Si-I also transforms partly to a-Si, as suggested by the broad peaks at 150 cm^{-1} and 470 cm^{-1}. Metastable Si-III (387 cm^{-1}) and a-Si can revert to polycrystalline Si-I after annealing. Therefore, we assume that the crystallization of a-Si is responsible for the decrease of the sub-band-gap absorption after annealing (see Fig. 3). The transformation from Si-III (387 cm^{-1}) back to polycrystalline Si-I corresponds to the configuration transformation of doped O atoms from the interstitial configuration of the lowest energy atoms to the quasi-substitutional and interstitial configurations of the higher energies doped atoms, resulting in the increase of the observed sub-band-gap absorptance with the annealing temperature.

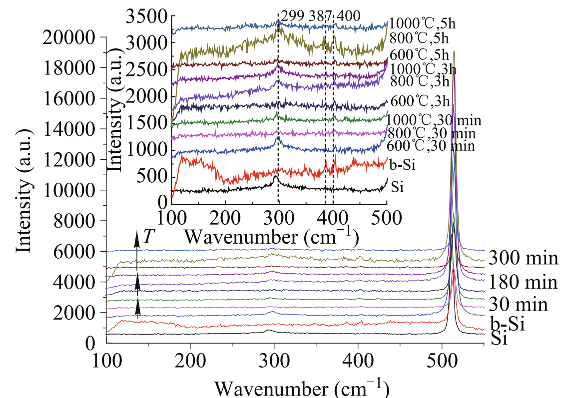

Fig. 6 Raman spectra of b-Si before and after annealing. The inset shows a detailed view of the spectrum from 100 to 500 cm^{-1}.

For the dependence of the optical absorptance of b-Si on the annealing time in the wavelength range of 1200–2500 nm, we propose the structural transformations of doped silicon as a probable cause of the deactivation of the sub-band-gap absorption. Here, the structural transformations, by which quasi-substitutional and higher energies interstitial configurations transform into the lowest interstitial configurations, differ from that discussed above. When annealing at lower temperature (600 and 800 °C), substitutional configurations are very stable, and quasi-substitutional and higher energies interstitial configurations have a better stability than those annealed at higher temperature, so that the transformation occurs at a small extent regardless of the du-

Frontiers of Physics

ration of the annealing time; thus, the absorptance is almost invariant with the annealing time, as shown in Fig. 5(a). Conversely, when annealing at the higher temperature of 1000 °C, quasi-substitutional oxygen atoms oscillate strongly around the lattice positions and the silicon atoms largely diffuse in the interstitial, causing the transformation from quasi-substitutional and higher energies substitutional configurations to lowest interstitial configuration, for longer annealing time, and thus reducing the sub-band-gap absorption. The configurations distribution would progressively equilibrate. Therefore, the sub-band-gap absorptance decreases with the annealing time and tend to the stabilization, as shown in Fig. 5(b).

Certainly, in the actual annealing process, both the deactivation and reactivation of the sub-band-gap absorptance always occur simultaneously by diffusion and the dominance of either depends on the annealing conditions. However, in our experiments, a maximum value of about 30% in sub-band-gap absorptance of b-Si was obtained after annealing at 1000 °C for 30 min, which is the best condition for the annealing process.

4 Summary

In summary, we have studied the surface morphology and optical characteristics of microstructured b-Si produced by femtosecond laser as a function of different annealing conditions in vacuum. The annealing process reduces the lattice defects and suppresses the light trapping, causing the increase of the reflectance and transmittance and a slight decrease of the absorptance. However, the annealing can restore many defects on the surface, which can greatly reduce the density of the recombination centers and enhance the mobility of the carriers. The sub-band-gap absorptance of b-Si varies not only with the wavelength, but also with the annealing temperature and time duration. Annealing may cause the deactivation and reactivation of the sub-band-gap absorptance by diffusion; the dominant effect depends on the annealing conditions. The deactivation of the sub-band-gap absorptance with the annealing temperature in the range of 1200–1500 nm is explained by using the partial restoration of the damaged lattices, while the sub-band-gap absorptance in the region above 1500 nm is reactivated by the structural transformations from the quasi-substitutional to the substitutional configurations. Regarding the deactivation of the sub-band-gap absorption of b-Si for longer annealing time in the wavelength region of 1200–2500 nm, a probable cause is the transformation from the quasi-substitutional and higher energies interstitial configurations to the lowest energy interstitial configurations through high-temperature annealing for a longer time. A maximum value of about 30% in sub-band-gap absorptance of b-Si was obtained after annealing at 1000 °C for 30 min, which is the best condition for the annealing process in our experiments. Therefore, a feasible way to obtain micro and nanoscale silicon material with higher controllable properties is provided in this paper.

Acknowledgements This work was supported by the National Basic Research Program of China (Grant No. 2012CB934201), Tianjin Research Program of Application Foundation and Advanced Technology (Grant No. 12JCYBJC10900), and the Natural Science Foundation of Guangdong Province (Grant No. S2013010012022).

References

1. T. H. Her, R. J. Finlay, C. Wu, S. Deliwala, and E. Mazur, Microstructuring of silicon with femtosecond laser pulses, *Appl. Phys. Lett.* 73(12), 1673 (1998)
2. R. Younkin, J. E. Carey, E. Mazur, J. A. Levinson, and C. M. Friend, Infrared absorption by conical silicon microstructures made in a variety of background gases using femtosecond-laser pulses, *J. Appl. Phys.* 93(5), 2626 (2003)
3. T. H. Her, R. J. Finlay, C. Wu, and E. Mazur, Femtosecond laser-induced formation of spikes on silicon, *Appl. Phys., A Mater. Sci. Process.* 70(4), 383 (2000)
4. M. Y. Shen, C. H. Crouch, J. E. Carey, R. Younkin, E. Mazur, M. Sheehy, and C. M. Friend, Formation of regular arrays of silicon microspikes by femtosecond laser irradiation through a mask, *Appl. Phys. Lett.* 82(11), 1715 (2003)
5. M. Y. Shen, C. H. Crouch, J. E. Carey, and E. Mazur, Femtosecond laser-induced formation of submicrometer spikes on silicon in water, *Appl. Phys. Lett.* 85(23), 5694 (2004)
6. D. Tran, Y. C. Lam, H. Zheng, V. Murukeshan, J. Chai, and D. E. Hardt, Femtosecond laser processing of crystalline silicon (2005)
7. H. M. Branz, V. E. Yost, S. Ward, K. M. Jones, B. To, and P. Stradins, Nanostructured black silicon and the optical reflectance of graded-density surfaces, *Appl. Phys. Lett.* 94(23), 231121 (2009)
8. T. Chen, J. Si, X. Hou, S. Kanehira, K. Miura, and K. Hirao, Luminescence of black silicon fabricated by high-repetition rate femtosecond laser pulses, *J. Appl. Phys.* 110(7), 073106 (2011)
9. J. T. Sullivan, R. G. Wilks, M. T. Winkler, L. Weinhardt, D. Recht, A. J. Said, B. K. Newman, Y. Zhang, M. Blum, S. Krause, W. L. Yang, C. Heske, M. J. Aziz, M. Bär, and T. Buonassisi, Soft x-ray emission spectroscopy studies of the electronic structure of silicon supersaturated with sulfur, *Appl. Phys. Lett.* 99(14), 142102 (2011)
10. M. T. Winkler, M. J. Sher, Y. T. Lin, M. J. Smith, H. Zhang, S. Gradečak, and E. Mazur, Studying femtosecond-laser hy-

perdoping by controlling surface morphology, *J. Appl. Phys.* 111(9), 093511 (2012)

11. Z. D. Chen, Q. Wu, M. Yang, J. H. Yao, R. A. Rupp, Y. A. Cao, and J. J. Xu, Time-resolved photoluminescence of silicon microstructures fabricated by femtosecond laser in air, *Opt. Express* 21(18), 21329 (2013)
12. C. Wu, C. H. Crouch, L. Zhao, J. E. Carey, R. Younkin, J. A. Levinson, E. Mazur, R. M. Farrell, P. Gothoskar, and A. Karger, Near-unity below-band-gap absorption by microstructured silicon, *Appl. Phys. Lett.* 78(13), 1850 (2001)
13. J. E. Carey, C. H. Crouch, and E. Mazur, Femtosecond-laser-assisted microstructuring of silicon surfaces, *Opt. Photonics News* 14(2), 32 (2003)
14. J. E. Carey and E. Mazur, Femtosecond laser-assisted microstructuring of silicon for novel detector, sensing and display technologies, in: Lasers and Electro-Optics Society, 2003 (LEOS 2003). The 16th Annual Meeting of the IEEE, 481 (2003)
15. B. K. Nayak, V. V. Iyengar, and M. C. Gupta, Efficient light trapping in silicon solar cells by ultrafast-laser-induced self-assembled micro/nano structures, *Prog. Photovolt. Res. Appl.* 19(6), 631 (2011)
16. Z. D. Chen, Q. Wu, M. Yang, B. Tang, J. H. Yao, R. A. Rupp, Y. A. Cao, and J. J. Xu, Generation and evolution of plasma during femtosecond laser ablation of silicon in different ambient gases, *Laser Part. Beams* 31(03), 539 (2013)
17. L. Nesbit, Annealing characteristics of Si-rich SiO_2 films, *Appl. Phys. Lett.* 46(1), 38 (1985)
18. S. Kosowsky, P. S. Pershan, K. Krisch, J. Bevk, M. Green, D. Brasen, L. Feldman, and P. Roy, Evidence of annealing effects on a high-density Si/SiO_2 interfacial layer, *Appl. Phys. Lett.* 70(23), 3119 (1997)
19. G. Ghislotti, B. Nielsen, P. Asoka-Kumar, K. Lynn, A. Gambhir, L. Di Mauro, and C. Bottani, Effect of different preparation conditions on light emission from silicon implanted SiO_2 layers, *J. Appl. Phys.* 79(11), 8660 (1996)
20. C. Wu, C. H. Crouch, L. Zhao, and E. Mazur, Visible luminescence from silicon surfaces microstructured in air, *Appl. Phys. Lett.* 81(11), 1999 (2002)
21. J. E. Carey, C. H. Crouch, M. Shen, and E. Mazur, Visible and near-infrared responsivity of femtosecond-laser microstructured silicon photodiodes, *Opt. Lett.* 30(14), 1773 (2005)
22. R. A. Myers, R. Farrell, A. M. Karger, J. E. Carey, and E. Mazur, Enhancing near-infrared avalanche photodiode performance by femtosecond laser microstructuring, *Appl. Opt.* 45(35), 8825 (2006)
23. T. G. Kim, J. M. Warrender, and M. J. Aziz, Strong sub-band-gap infrared absorption in silicon supersaturated with sulfur, *Appl. Phys. Lett.* 88(24), 241902 (2006)
24. M. A. Sheehy, L. Winston, J. E. Carey, C. M. Friend, and E. Mazur, Role of the background gas in the morphology and optical properties of laser-microstructured silicon, *Chem. Mater.* 17(14), 3582 (2005)
25. B. R. Tull, M. T. Winkler, and E. Mazur, The role of diffusion in broadband infrared absorption in chalcogen-doped silicon, *Appl. Phys. A, Mater. Sci. Process.* 96(2), 327 (2009)
26. B. K. Newman, M. J. Sher, E. Mazur, and T. Buonassisi, Reactivation of sub-bandgap absorption in chalcogen-hyperdoped silicon, *Appl. Phys. Lett.* 98(25), 251905 (2011)
27. M. J. Smith, Y. T. Lin, M. J. Sher, M. T. Winkler, E. Mazur, and S. Gradečak, Pressure-induced phase transformations during femtosecond-laser doping of silicon, *J. Appl. Phys.* 110(5), 053524 (2011)
28. B. K. Newman, E. Ertekin, J. T. Sullivan, M. T. Winkler, M. A. Marcus, S. C. Fakra, M. J. Sher, E. Mazur, J. C. Grossman, and T. Buonassisi, Extended X-ray absorption fine structure spectroscopy of selenium-hyperdoped silicon, *J. Appl. Phys.* 114(13), 133507 (2013)
29. H. Shao, Y. Li, J. Zhang, B. Y. Ning, W. Zhang, X. J. Ning, L. Zhao, and J. Zhuang, Physical mechanisms for the unique optical properties of chalcogen-hyperdoped silicon, *Europhys. Lett.* 99(4), 46005 (2012)
30. J. Zhu, G. Yin, M. Zhao, D. Chen, and L. Zhao, Evolution of silicon surface microstructures by picosecond and femtosecond laser irradiations, *Appl. Surf. Sci.* 245(1–4), 102 (2005)